Sains Malaysiana 39(5)(2010): 837–844

Enhancement of the Production Yield of Fluorescent Silicon Nanostructures Using Silicon-Based Salts

(Peningkatan Hasil Pengeluaran Nanostruktur Silikon Berpendarfluor Menggunakan Garam Berasaskan Silikon)

LAILA H. ABUHASSAN*

ABSTRACT

The increase in the amount of extracted silicon nanostructures resulting from the incorporation of sodium metasilicon salt in the etching solution was investigated. Silicon nanostructures were prepared in the form of thin fluorescent films via anodisation etching of silicon wafers in aqueous HF/H_2O_2 solution in the presence of the silicon-based salt. The quality of the fluorescent films was assessed using several nondestructive analytical techniques. The nanostructures produced were then extracted. The harvested nanostuctures were examined for quantitative elemental analysis using atomic absorption spectrophotometry. This investigation was limited to silicon nanostructures with size ≤ 200 nm. The results indicate that the incorporation of the silicate increased the yield of silicon nanostructures production significantly.

Keywords: Nondestructive characterisation; nanomaterial; silicate; silicon nanostructures

ABSTRAK

Peningkatan amaun nanostruktur silikon yang diperolehi hasil gabungan garam natrium metasilikon di dalam larutan punaran telah dikaji. Nanostruktur silikon disediakan dalam bentuk filem nipis pendarfluor melalui punaran penganodan wafer silikon di dalam larutan akueus HF/H_2O_2 dengan kehadiran garam silikon. Kualiti filem pendarfluor dinilai menggunakan beberapa teknik analisis tanpa musnah. Nanostruktur yang dihasilkan dilakukan analisis kuantitatif bagi unsur-unsur mengggunakan spektrofotometri serapan atom. Kajian ini dihadkan kepada nanostruktur silikon bersaiz ≤ 200 nm. Keputusan menunjukkan kehadiran silikat telah meningkatkan hasil pengeluaran nanostruktur silikon dengan signifikan.

Kata kunci: Nanobahan; nanostruktur silikon; pencirian tanpa musnah, silikat

INTRODUCTION

Over the last fifteen years, a variety of methods and source materials have been used to synthesize silicon nanostructures. Risbud et al. (1993) used silicon powder dispersed in the viscous melt to produce nanometer sized silicon trapped in a glass matrix; ion implantation and subsequent thermal annealing were used to produce Si, Ge, and Si-Ge nanocrystals in SiO_2 (Zhu et al. 1995). Implantation of silicon ions through apertures opened in a stencil-mask was used to create silicon nanoparticles within a thin layer of SiO_2 (Dumas et al. 2007). Direct dc sputtering of silicon material onto a liquid nitrogen-cooled stainless-steel trap was also used to prepare silicon nanoparticles (Zhu et al. 2000). Laser-induced pyrolysis was also shown to produce silicon nanoparticles (Di Nunzio & Martelli 2006; Swihart et al. 2003). Silicon nanoparticles were prepared from polycrystalline silicon by an arc discharge method in liquid nitrogen (Kobayashi et al. 2006). Spark ablation from crystalline silicon substrate was used to produce nanometer-scale silicon clusters (Saunders et al. 1993). Nanometer-sized silicon crystallites were prepared using laser ablation combined with constant pressure gas evaporation (Yoshida et al. 1996). Plasma-enhanced chemical vapor deposition was used to produce nanocrystalline silicon films (Kumar et al. 2008). Holmes et al. 2001 prepared silicon nanocrystals by thermally degrading diphenylsilane in mixtures of octanol and hexane. Submicrometer-sized silicon single crystals were fabricated using reduction of $SiCl_4$ and $RSiCl_3$ (R = H, octyl) by sodium metal (Heath 1992). Silicon nanocrystals were produced by sodium naphthalenide reduction of silicon tetrachloride/silicon halides (Baldwin et al. 2002a, 2002b). Hydrogen-capped silicon nanoparticles were prepared by the metathesis reaction of NaSi with NH_4Br (Zhang et al. 2007). Silicon nanocrystals were also prepared by bromine oxidation of porous silicon followed by reaction with butyllithium (Carter et al. 2005).

The production of silicon nanostructures using chemical etching of elemental silicon has been widely adopted. Colloidal silicon nanocrystallites were prepared by sonication of anodically etched p-doped silicon and n-doped silicon (Sweryda-Krawiec et al. 1999a). Ultrasonic dispersion of thin sections of porous silicon in organic solvents was used to produce silicon nanoparticles

(Bley et al. 1996). Electrochemical etching of silicon wafers was used to produce porous silicon (Yamani et al. 1997) or dispersions of silicon nanoparticles (Nayfeh et al. 2003; Nielsen et al. 2007). In all such procedures, a positively biased silicon wafer is electrochemically etched in an HF/H_2O_2 solution. Numerous applications such as nanomemory and painting interior walls of buildings were enabled by these developments. However, the production of macroscopic, low cost amounts of Si nanostructures is a basic requirement for their commercial viability.

We previously studied the synthesis of silicon nanomaterial from sodium metasilicon salt (Na_2SiO_3) (Abuhassan & Nayfeh 2005, 2007). In this method, silicon nanomaterial was electrodeposited on a positively-biased platinum, or platinum coated silicon, substrate that was immersed in an HF/H_2O_2/silicate aqueous solution. Although the process is advantageous because the silicates are an abundant low cost source of silicon, the procedure is electrodeposition-based, and therefore limited to deposition on conducting and semiconducting substrates. We recently investigated the integration of the two methods, electrochemical etching and silicate electrodeposition. Through analysis of the area under the corresponding peaks in the infrared (IR) absorption spectra, an increase in the amount of the Si nanomaterial was observed due to the incorporation of the silicon-based salt in the etching solution (Abuhassan 2009). This effect was found to depend on the volume of the silicate solution added to the etchants. It is worth mentioning that this study was performed on the Si nanostructures present within the porous Si network, i.e. while the synthesized nanomaterial was still residing on the silicon substrate. In terms of analysis, all the resulting silicon species were included in the measured IR signal.

In this paper, we investigated the effect of integrating an electrodeposition with electrochemical etching techniques on the net amount of Si nanostructures produced. The results of this study, however, are largely limited to Si nanostructures of size ≤ 200 nm that were extracted from the porous silicon network. A volume of aqueous 1 mg/L metasilicate solution was selected such that sampled nanomaterial was mostly hydrogen terminated. To satisfy this requirement, the IR absorption spectra of the samples were used with the area under the corresponding peak as an indicator to the amount of the absorbing species present. Consequently, the sample whose IR spectrum showed a ratio of the area under the absorption peak at about 2100 cm^{-1} (characteristic of stretching monohydrides with reconstructed Si-Si bonds, i.e. corresponding to the major functional states present in Si nanomaterial) to that under 1100 cm^{-1} (corresponding to oxygen stretching signal of Si-O-Si and was observed for silicon nanoclusters) larger than unity was chosen. Based upon the results of the previous study and taking this criterion into consideration, 15 mL of the silicate solution was used in this work. Before proceeding to extraction, filtration, and quantitative elemental analysis of the synthesized nanostructures, the quality of the fluorescent porous film was assessed and the abovementioned criterion tested. The results show that the integration of elctrodeposition and electrochemical etching techniques has a synergetic effect of boosting the overall yield of production of the silicon nanomaterial.

Method

A device quality p-doped (111) silicon wafer of resistivity 4-8 ohm.cm was cleaned, rinsed in doubly deionised water, and sonicated in methanol. Etching solution was prepared from a mixture of 48-51% HF (5 mL), 50% H_2O_2 (15 mL), analytical methanol (10 mL), and 15mL of 1mg/liter metasilicate water solution ($Na_2SiO_3.5H_2O$). A portion of the silicon wafer (~1 cm^2) was then immersed in the etching solution, and a platinum wire electrode was placed ~ 1 cm away from, and opposite to the silicon substrate. The silicon wafer was positively biased with respect to the counter platinum wire electrode. A constant current density of ~ 10 mA/cm^2 was drawn for one hour, after which the current was stopped and the silicon substrate removed, rinsed in doubly deionised water, and dried off in nitrogen atmosphere. The emission of the synthesized film was tested using a UV excitation source at 365 nm. In order to isolate the effect of incorporating the silicon salt in the etching solution, a control/reference sample was prepared following the same procedure and under similar conditions, however the etching solution did not contain the silicon salt.

In order to assess the quality and reproducibility of the fabricated fluorescent films, and before proceeding to the extraction and analysis of the nanomaterial, routine nondestructive analyses were undertaken. These include characterisation via Fourier transform infrared spectroscopy (FTIR) and fluorescent microscope imaging under ultraviolet (UV) illumination. First, the samples were characterised for molecular infrared activity using FTIR. The transmission infrared spectra were recorded using a Nicolet (Impact 400) FTIR spectrometer with an Ever-GloTM mid-IR source, a DTGS detector, and a nitrogen purged sample chamber. The IR spectra were converted from transmittance to absorbance units, which were then used to identify the functional groups present. Particular attention was given to the relative abundance of hydrogen terminated, as compared to oxygen bonded, silicon nanostructures. As mentioned earlier, the area under the peak in the IR spectrum was used as an indicator to the amount of the corresponding absorbing species present in the sample. The IR spectrum demonstrated that most of the fabricated silicon nanostructures were hydrogen terminated in the case of the sample which was prepared using 15 mL of the silicate solution. As the choice of the sample (i.e. the amount of silicate solution used during the synthesis process) proved adequate, we proceeded to the second step. The samples were imaged for luminescent activity using a fluorescent microscope from Leica. Images from the fluorescent microscope were taken under UV 365

nm wavelength incoherent illumination. Additionally, structural and compositional analyses of these films were performed using scanning electron microscopy (SEM) and energy dispersive X-ray analysis (EDAX). For these analyses, a Quanta 600 scanning electron microscope that is equipped with an EDAX attachment was used.

We also examined the production yield of the silicon nanomaterial with and without incorporating the metasilicate in the etching solution. For this purpose, the synthesized material was ultrasonically shaken out from the silicon substrate in 5 mL of analytical methanol. The extracted material was redispersed into 5 mL of doubly deionised water after evaporating the methanol. Entities larger than 200 nm were filtered out. Atomic absorption spectrophotometry was then used to measure the amount of silicon present in the prepared colloid using SOLAAR M Series from Thermo Elemental. In order to determine the concentration of silicon in the samples and reference, the absorption values of the spectrophotometer were first calibrated versus concentration (ppm) using standard silicon solution. Then the measured absorption values were converted into concentrations (ppm) using the calibration curve. The results were normalised to the area of the substrate from which the nanomaterial was harvested. To ensure reproducibility, the experiment was repeated several times. Eight sample "replicates" were synthesized using silicate/acid/peroxide solution and eight replicates of the control/reference were prepared in acid/peroxide solution. The concentration of silicon in the synthesized nanomaterial was then measured for each sample twice and an average value was determined. The average concentration of silicon was used as an indicator to the production yield of silicon nanomaterial. Finally, the enhancement factor was calculated from the percentage increment in the concentration of silicon that resulted from adding the silicate to the etching solution.

RESULTS AND DISCUSSION

All the samples that were synthesized under similar conditions exhibited similar optical, structural and compositional characteristics. These results were in agreement with our previous investigation (Abuhassan 2009). Consequently, only representative results are shown for demonstration purposes. For each characterisation technique, two spectra/images were displayed. The first (referred to as (a)) corresponds to the sample prepared using the silicate solution, whereas the second (referred to as (b)) corresponds to the reference/control.

The FTIR spectra in Figure 1 show the absorption peaks to the corresponding molecular vibrations of Si-H or Si-Si bulk vibrations at 615-619 cm^{-1} and 623 cm^{-1}, $Si-H_2$ scissors or $Si-H_3$ symmetric or antisymmetric deformation at 905-910 cm^{-1}. The absorption in the 1100 cm^{-1} region corresponds to the oxygen stretching signal of Si-O-Si. The shoulder that appears at 1200 cm^{-1} corresponds to O-C signal. The peaks in the range 2070-2090 cm^{-1} are characteristic of other stretching monohydrides (coupled H-Si-Si-H or H attached to Si atoms with Si-Si bonding arrangements different than for bulk Si). The broad peak in this range of the spectrum may be due to the presence of other hydrides, i.e. SiH_x. Comparison between the spectra of the samples, prepared using Si-based salt in HF/H_2O_2 aqueous solution, and those of the control/reference demonstrates an obvious enhancement of the features absorbing at and near 1100 and 2070 cm^{-1}.

Since the recorded transmission IR spectrum measures an integrated signal across the entire wafer, subtraction of spectra may be used to isolate the signal from the additionally formed absorbing entities in the luminescent thin porous layer. Figure 2 shows the subtraction result; hence the IR absorption spectrum corresponds to the species that were produced due to incorporating the silicon

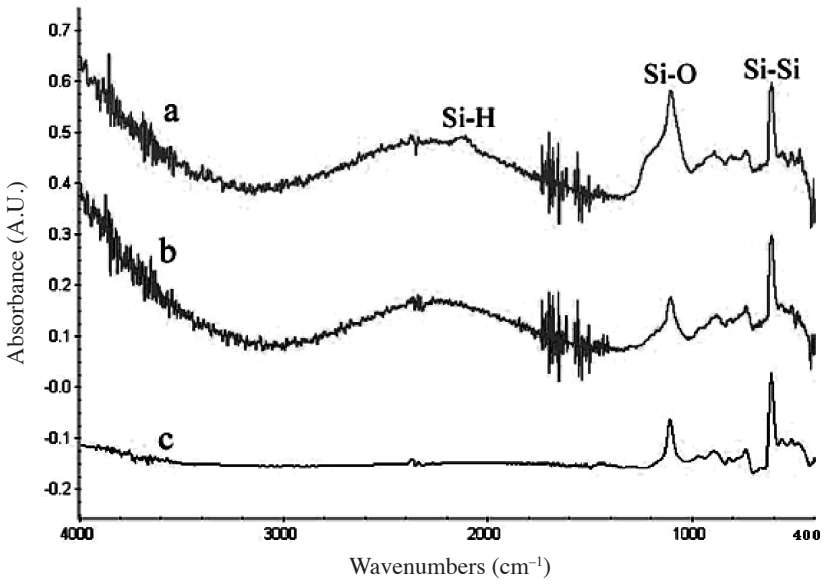

FIGURE 1. FTIR spectra of (a) sample prepared using Si-based salt in HF/H_2O_2 aqueous solution, (b) control sample and (c) silicon substrate

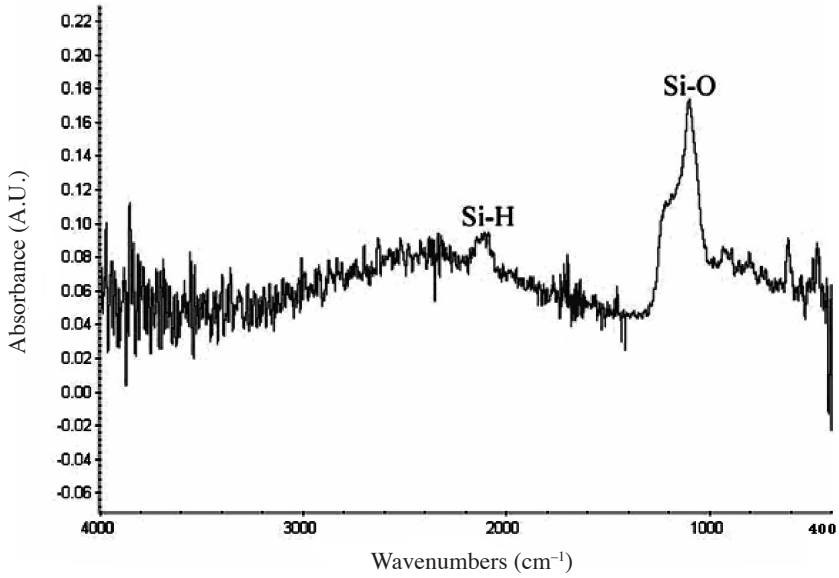

FIGURE 2. The subtraction of the FTIR spectrum of the control sample from that of the sample prepared using the silicate/HF/ H_2O_2 solution

salt in the etching solution. The main absorption modes that appear in this spectrum are around: 620, 1100, and 2070 cm^{-1}. The main peak near 1100 cm^{-1} and that about 620 cm^{-1} were previously observed for the silicon nanoclusters in porous silicon (Sweryda-Krawiec et al. 1999b). The shoulder at about 1200 cm^{-1} was assigned to the C-O signal (Cabaniss et al. 1995). The absorption features around 2070 cm^{-1} are characteristic of stretching monohydrides with reconstructed Si-Si bonds, and indicate the presence of the major bonding states present in silicon nanoparticles, as these particles are composed of a silicon core with H-terminated reconstructed silicon surface (Nayfeh et al. 2003; Mitas et al. 2001). Accordingly, the IR results indicate the production of extra Si nanomaterial due to the incorporation of the silicon salt in the etching solution. As the area under the peak at about 2100 cm^{-1} (corresponding to the major functional states present in Si nanomaterial) to that under 1100 cm^{-1} (corresponding to oxygen stretching signal of Si-O-Si and was observed for silicon nanoclusters) was larger than unity, one may conclude that the fabricated silicon nanostructures were mainly hydrogen terminated. These results were in agreement with our previous study (Abuhassan 2009). In addition, the O-C signal, at 1200 cm^{-1}, has been enhanced as a result of adding the salt to the etching solution. This result may explain the lower degree of homogeneity and higher roughness observed in the fluorescent microscope (Figure 3a-b) and SEM (Figure 4a-b) images of the samples, as they have extra bonding states present within the porous network.

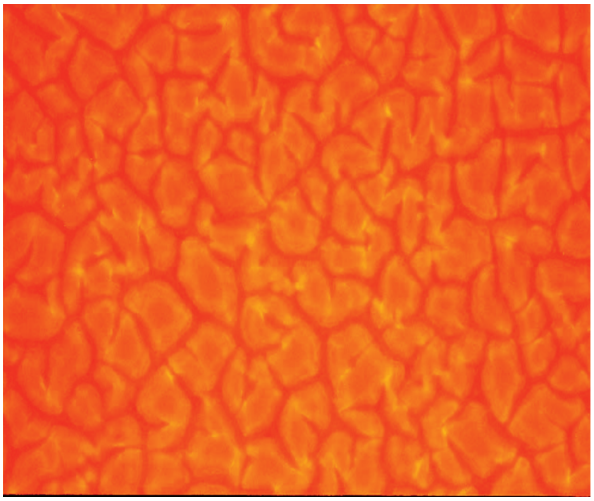

FIGURE 3a. Fluorescent microscope image of the central part of the sample prepared in silicate/HF/ H_2O_2 solution (see online version for colours)

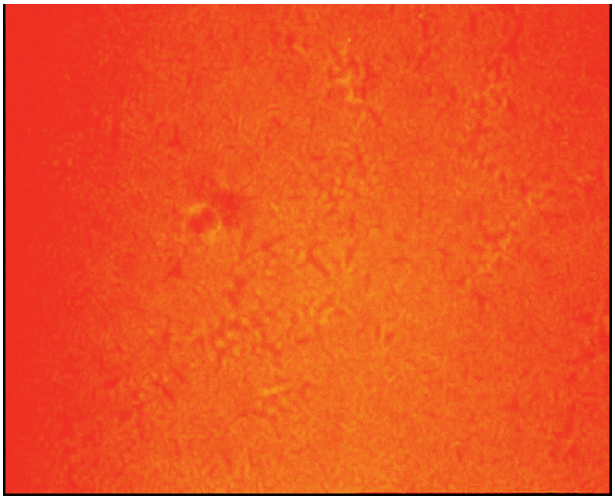

FIGURE 3b. Fluorescent microscope image of the central part of the control sample (see online version for colours)

Under UV exposure, both the sample and the control demonstrated strong fluorescence activity in the orange-red region of the spectrum as well as high photostability. Images from the fluorescent microscope, taken under 365 nm excitation and similar conditions of magnification, are shown in Figure 3a-b. These images correspond to similar regions of the tested samples. Both images show strong fluorescence activity in the orange-red region of the spectrum. In both cases, the images indicate that the fluorescent network is composed of optically active material. Direct comparison between the two images showed that the roughness of the fluorescent material is higher in the case of the sample that was synthesized in the silicate/HF/H_2O_2 solution (Figure 3a). The increased roughness observed may be due to the extra features present, as mentioned in the above paragraph. However, these results were in agreement with our previous study (Abuhassan 2009).

Surface microstructural characterisation via SEM images was shown in Figure 4a-b for the samples under investigation. The white/black colours in these figures indicate material/void, respectively. The large white areas observed in the sample's image (Figure 4a) is a clear indication towards coagulation of the particles when the salt was added to the etching solution. Comparison of Figure 4a and Figure 4b. show that the surface layer of the reference sample was more homogeneous than that of the sample prepared using the silicate/acid/peroxide etchant. This is to be expected as the latter sample had additional entities due to the incorporation of the silicate into the etching solution. However, the porous fluorescent network was previously found to be composed of ~3-6 nm sized structures whether using silicate/acid/peroxide or peroxide/acid etchants (Abuhassan & Nayfeh 2007). Furthermore, Si nanostructures prepared via electrodeposition from the silicate solution

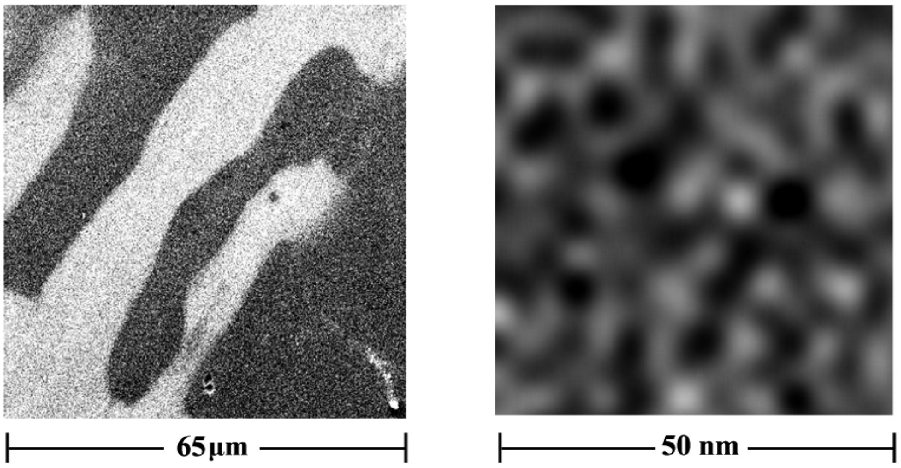

FIGURE 4a. SEM image of the center of the sample prepared in the silicate/HF/H_2O_2 solution using two values of magnification. The appropriate scales are indicated on the figures

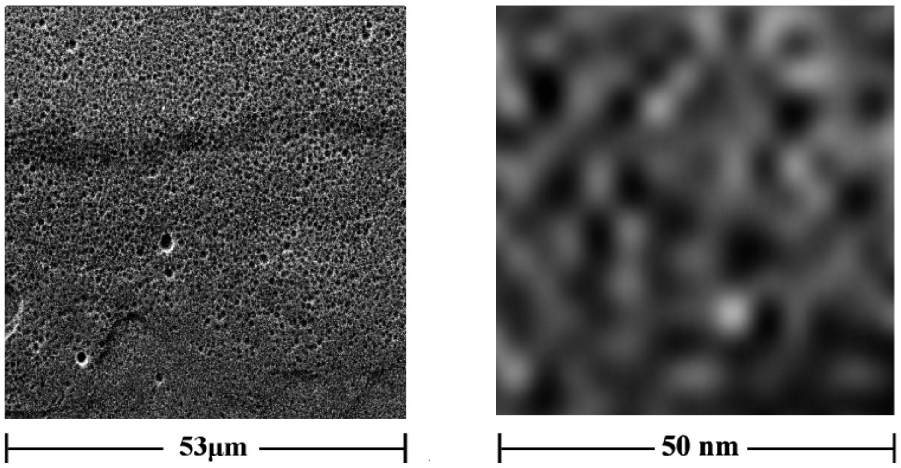

FIGURE 4b. SEM image of the center of the sample prepared in silicate/HF/H_2O_2 solution using two values of magnification. The white / black colors indicate the material / void, respectively. The appropriate scales are indicated on the figures

were previously shown to have similar range of size (Abuhassan & Nayfeh 2005).

The elemental content of the produced material was investigated using the EDAX spectrum of the fluorescent film. Figure 5 shows the EDAX spectrum for the same region whose SEM image was shown in Figure 4a. This spectrum is similar to that of the control sample. In both cases, the fluorescent nanomaterial was composed mainly of silicon with less than 1% of other elements such as oxygen, fluorine, potassium and sodium. This is in agreement with the above IR results.

Finally, the enhancement of the silicon nanomaterial production yield was examined via the concentration of silicon present in the resulting nanomaterial after being extracted from the substrate, dispersed in similar volumes of deionized water, and normalized to the etched area of the substrate. The values of the concentration, as measured using atomic absorption spectrophotometry and after being normalized to the etched area of the substrate, for the samples and the corresponding control/reference are shown in Tables 1 and 2, respectively. An average concentration value of 5.43 ± 0.82 ppm was found in the case of samples prepared in silicate/acid/peroxide solution. Whereas an average value of 3.51 ± 0.64 ppm was obtained for the control/reference samples. These results indicate a significant enhancement of the silicon nanomterail production yield due to the integration of the silicon-based salt into the etching solution. The enhancement factor was found to be (55 ± 13)%. This enhancement effect is expected since the incorporated silicon-based salt forms an additional source of the silicon nanomaterial. It is important here to mention that the amount of the silicate solution used during the fabrication process may play a crucial role, as dissolution of the produced material may take place (Abuhassan 2009).

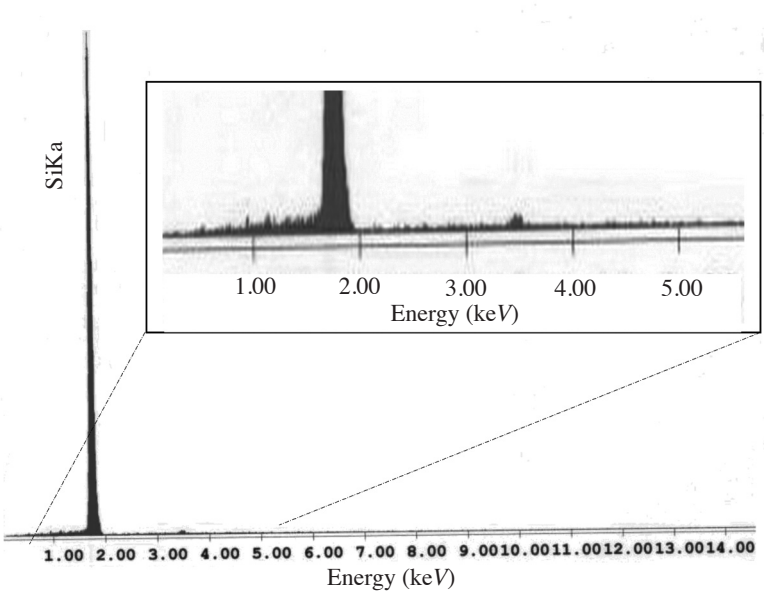

FIGURE 5. EDAX spectrum of the sample prepared using Si-based salt in HF/H_2O_2 aqueous solution. The inset is an enlargement of a section of the figure

TABLE 1. Measurements of silicon nanomaterial concentration (ppm) in the samples prepared using silicate/acid/peroxide solution

Sample Number	Concentration (ppm)			
	First Trial	Second Trial	Average	Deviation
Sample 1	6.1	5.4	5.75	0.43
Sample 2	4.6	4.1	4.35	-1.08
Sample 3	4.8	5.0	4.90	-0.53
Sample 4	5.2	4.5	4.85	-0.58
Sample 5	4.7	5.4	5.05	-0.38
Sample 6	5.1	5.7	5.40	-0.03
Sample 7	6.3	6.4	6.35	0.92
Sample 8	6.7	6.8	6.75	1.32
Average concentration	5.43 ± 0.82			

TABLE 2. Measurements of silicon nanomaterial concentration (ppm) in the control/reference samples prepared using acid/peroxide solution

Sample Number	Concentration (ppm)			
	First Trial	Second Trial	Average	Deviation
Control 1	3.3	2.4	2.85	-0.66
Control 2	3.4	4.0	3.70	0.91
Control 3	3.4	4.1	3.75	0.24
Control 4	2.9	3.4	3.15	-0.36
Control 5	4.4	4.4	4.40	0.89
Control 6	4.0	2.7	3.35	-0.16
Control 7	4.3	3.7	4.00	0.49
Control 8	3.0	2.8	2.90	-0.61
Average concentration		3.51 ± 0.64		

CONCLUSION

In conclusion, we observed that the incorporation of the silicon-based salt in the electrochemical etching HF/H_2O_2 aqueous solution enhanced the production yield of silicon nanostructures. The resulting nanomaterial was shown to be composed mainly of hydrogen terminated Si nanostructures with less than 1% of other elements. Quantitative elemental analysis was performed on the extracted Si nanostructures, with size ≤ 200 nm. After normalisation with respect to the area of the substrate, we found that the addition of the silicate to the etching solution enhanced the production yield of silicon nanostructures by significant proportions.

ACKNOWLEDGEMENTS

This work has been supported by the University of Jordan. The author is indebted to Professor Munir Nayfeh for his invaluable comments during the preparation of this manuscript, and gratefully acknowledges Mr. Osama Taqatqa and Ms. Asma Al-Rifai for their technical assistance.

REFERENCES

Abuhassan, L.H. 2009. Optimization of Fluorescent Silicon Nanomaterial Production Using Peroxide/Acid/Salt Technique. *Sains Malaysiana* 38: 77-83.

Abuhassan, L.H. & Nayfeh, M.H. 2005. Electrodeposition of fluorescent Si nanomaterial from acidic sodium silicate solutions. *Mat. Res. Soc. Symp. Proc.* 862. A8: 10.

Abuhassan, L.H. & Nayfeh, M.H. 2007. Material analysis of fluorescent Si nanomaterial prepared electrochemically from sodium silicate water glass solutions. *Dirasat* 34: 183-191.

Baldwin, R.K., Pettigrew, K.A., Garno, J.C., Power, P.P., Liu, G-Y. & Kauzlarich, S.M. 2002a. Room Temperature Solution Synthesis of Alkyl-Capped Tetrahedral Shaped Silicon Nanocrystals. *J. Am. Chem. Soc.* 124: 1150-1151.

Baldwin, R.K., Pettigrew, K.A., Ratai, E., Augustine, M.P. & Kauzlarich. S.M. 2002b. Solution reduction synthesis of surface stabilized silicon nanoparticles. *Chem. Commun.* 1822-1823.

Bley, R.A., Kauzlarich, S.M., Davis, J.E. & Lee, H.W.H. 1996. Characterization of Silicon Nanoparticles Prepared from Porous Silicon. *Chem. Mater.* 8: 1881-1888.

Cabaniss, Stephen, E. & McVey, lain F. 1995. Aqueous infrared carboxylate absorbances: aliphatic monocarboxylates. *Spectrochimica Acta Part* A 51: 2385-2395.

Carter, R.S., Harley, S.J., Power, P.P. & Augustine, M.P. 2005. Use of NMR Spectroscopy in the Synthesis and Characterization of Air- and Water-Stable Silicon Nanoparticles from Porous Silicon. *Chem. Mater.* 17: 2932-2939.

Di Nunzio, P.E. & Martelli, S. 2006. Coagulation and Aggregation Model of Silicon Nanoparticles from Laser Pyrolysis. *Aerosol Science and Technology* 40: 724-734.

Dumas, C., Grisolia, J., Ressier, L., Arbouet, A., Paillard, V., Ben Assayag, G., Claverie, A., Van den Boogaart, M.A.F. & Brugger, J. 2007. Synthesis of localized 2D-layers of silicon nanoparticles embedded in a SiO_2 layer by a stencil-masked ultra-low energy ionimplantation process. *Phys. Stat. Sol.* A. 204: 487-491.

Heath, J.R. 1992. A liquid-solution-phase synthesis of crystalline silicon. *Science* 258(5085): 1131-1133.

Holmes, J.D. Ziegler, K.J. Doty, R.C. Pell, L.E. Johnston, K.P. & Korgel, B.A. 2001. Highly Luminescent Silicon Nanocrystals with Discrete Optical Transitions. *J. Am. Chem. Soc.* 123: 3743-3748.

Kobayashi, M., Liu, S-M., Sato, S., Yao, H. & Kimura, K. 2006. Optical Evaluation of Silicon Nanoparticles Prepared by Arc Discharge Method in Liquid Nitrogen. *Jpn. J. Appl. Phys.* 45: 6146-6152.

Kumar, S. Dixit, P.N. Rauthan, C.M.S. Parashar, A. & Gope, J. 2008. Effect of power on growth of nanocrystalline silicon films. *J. Phys.: Condens. Matter* 20: 335215 (7pp).

Mitas, L., Therrien, J., Twesten, R., Belomoin, G. & Nayfeh, M.H. 2001. Effect of surface reconstruction on the structural prototypes of ultrasmall ultrabright Si_{29} nanoparticles. *Appl. Phys. Lett.* 78: 1918-1920.

Nayfeh, M.H., Rogozhina, E.V. & Mitas, L. 2003. Synthesis, Functionalization and Surface Treatment of Nanoparticles, edited by Marie-Isabelle Baraton, 173-231. USA American Scientific Publishers.

Nielsen, D., Abuhassan, L.H., Alchihabi, M., Al-Muhanna, A., Host, J. & Nayfeh, M.H. 2007. Current-less Anodization of intrinsic silicon powder grains: Formation of fluorescent Si nanoparticles. *J. Appl. Phys.* 101: 114302 (3pp).

Risbud, S.H. Liu, L-C. & Shakelford, J.F. 1993. Synthesis and luminescence of silicon remnants formed by truncated glassmelt-particle reaction. *Appl. Phys. Lett.* 63: 1648-1650.

Saunders, W.A., Sercel, P.C., Lee, R.B., Atwater, H.A., Vahala, K.J., Flagan, R.C. & Escorcia-Aparcio, E.J. 1993. Synthesis of luminescent silicon nanoclusters by spark ablation. *Appl. Phys. Lett.* 63: 1549-1551.

Sweryda-Krawiec, B., Cassagneau, T. & Fendler, J.H. 1999a. Ultrathin Electroactive Junctions Assembled from Silicon Nanocrystallites and Polypyrrole. *Adv Mater.* 11 (Comm.): 659-664.

Sweryda-Krawiec, B., Cassagneau, T. & Fendler, J.H. 1999b. Surface Modification of Silicon Nanocrystallites by Alcohols. *J. Phys. Chem. B.* 103: 9524-9529.

Swihart, M.T., Li, X., He, Y., Kirkey, W., Cartwright, A.N., Sahoo, Y. & Prasad, P.N. 2003. High-Rate Synthesis and Characterization of Brightly Luminescent Silicon Nanoparticles with Applications in Hybrid Materials for Photonics and Biophotonics. *Proc. of SPIE-The International Society for Optical Engineering*. 5222: 108-117.

Yamani, Z., Thompson, W.H., Abuhassan, L.H. & Nayfeh, M.H. 1997. Ideal anodization of silicon. *Appl. Phys. Lett.* 70: 3404-3406.

Yoshida, T., Takeyama, S., Yamada, Y. & Mutoh, K. 1996. Nanometer-sized siliconcrystallites prepared by excimer laser ablation in constant pressure inert gas. *Appl. Phys. Lett.* 68: 1772-1774.

Zhang, X., Neiner, D., Wang, S., Louie, A.Y. & Kauzlarich, S.M. 2007. A new solution route to hydrogen-terminated silicon nanoparticles: synthesis, functionalization and water stability. *Nanotechnology* 18: 095601 (6pp).

Zhu, J.G., White, C.W., Budai, J.D., Withrow, S.P. & Chen, Y. 1995. Growth of Ge, Si, and SiGe nanocrystals in SiO_2 matrices. *J. Appl. Phys.* 78: 4386-4389.

Zhu, Y., Wang, H. & Ong, P.P. 2000. Strong and stable photoluminescence from sputtered silicon nanoparticles. *J. Phys. D: Appl. Phys.* 33: 1965-1968.

Department of Physics
Faculty of Science
University of Jordan
Jubeiha, Amman 11942
Jordan

*Corresponding author; email: L.abuhassan@ju.edu.jo

Received: 21 October 2008
Accepted: 30 December 2009